Journal of Applied Polymer Science

Starch foam material performance prediction based on a radial basis function artificial neural network trained by bare-bones particle swarm optimization with an adaptive disturbance factor

Ruting Xia,[1] Xingyuan Huang,[2] Mengshan Li[2,3]

[1]School of Mechanical Engineering, Taizhou University, Taizhou, Zhejiang 318000, China
[2]College of Mechanical and Electric Engineering, Nanchang University, Nanchang 330029, China
[3]College of Physics and Electronic Information, Gannan Normal University, Ganzhou, Jiangxi 341000, China
Correspondence to: M. Li (E-mail: jcimsli@163.com)

ABSTRACT: A novel model based on a radial basis artificial neural network and bare-bones particle swarm optimization tuned with adaptive disturbance factor for predicting the performances of starch-based foam materials was established. The ethylene–vinyl acetate/starch mass ratio, glycerin content, and $NaHCO_3$ content were used as the input variables, whereas the tensile strength and rebound rate were taken as the output variables of the model. The prediction results show that model predictions were in great accordance with the experimental values. The root mean square error of prediction and the correlation coefficients were 0.0256 and 0.9873; this indicated the good performance of the model. The model predicted that the tensile strength of the starch-based foam materials would decrease slowly with increasing glycerin content and showed a V-shaped variation with increasing $NaHCO_3$ content. The rebound rate increased with increasing glycerin content and presented an inverted V-shaped variation with increasing $NaHCO_3$ content. The predicted results were consistent with the experimental results. © 2016 Wiley Periodicals, Inc. J. Appl. Polym. Sci. **2016**, *133*, 44252.

KEYWORDS: classification; crosslinking; foams; theory and modeling

Received 3 May 2016; accepted 31 July 2016
DOI: 10.1002/app.44252

INTRODUCTION

Starch-based foam materials are important natural biodegradable materials. Their sheets or membranes provide products for processing various materials and can be used as raw materials for various packing materials. They have extensive application prospects and have attracted more and more attention in recent years.[1] Foam materials made of starch and ethylene–vinyl acetate (EVA) have various excellent characteristics, including good degradability, small density, good elasticity, and excellent heat insulation.[2,3] As a new good compound-packaging material, it is beneficial for relieving white pollution and highly appreciated by the industrial and academic world. To improve the mechanical properties, microstructure, and degradation properties of these materials, some crosslinking agents and plasticizer have often been mixed with starch to get starch-based foam materials with good comprehensive properties.[4–7] Many experiments on the composition of this starch-based foam material have been done in actual scientific research or industrial production to test the properties of the materials; this has enabled the optimized combination of the components and corresponding contents.[8,9] Nevertheless, both material acquisition experiments and sample testing have shown that the production of these materials is time consuming and effort consuming and has a low economic efficiency.[10,11] If there is a theoretical mathematical model that could analyze the influence of the material components and their contents on product performances, it could significantly reduce the experimental load and provide important theoretical support for experiments.[12–14]

In starch-based EVA foam materials, the analysis of the influence of the crosslinking agent and plasticizer contents on product performance could offer important theoretical support for the processing of similar materials.[15,16] Hence, a mathematical model of the influence of the EVA–starch mass ratio, crosslinking agent content, and plasticizer content on product performances is discussed in this article. Zeng and Sun[17] made great contributions to studies on the establishment of similar mathematical models. Therefore, a model based on a back-propagation (BP) artificial neural network (ANN) for the performance prediction of biological foam materials was established. According to research results, the neural network model has a high prediction precision. The predicted values are close

to experimental values. However, the BP ANN has some shortcomings: it has a slow local search and is easily caught in local extremum.[18,19] Moreover, the model depends greatly on training algorithms, and this restricts its applications.[20,21]

The radial basis function (RBF) ANN is one of the most used models, and it has been applied in various fields. However, the RBF ANN has various problems. For example, the performance is directly correlated with the optimization of network weights. Research has found that the training process could be viewed as the optimization of the basis function center, expansion constant, and connection weight. The nature of ANN training is the optimization of network parameters.[22,23] Naturally, researchers have tried various intelligent optimization algorithms in network training; these have included genetic algorithms, particle swarm optimization (PSO) algorithms, and fish swarm algorithms.[24,25]

Therefore, in this study, we attempted to establish an RBF ANN prediction model based on a bare-bones particle swarm optimization (BBPSO) algorithm, a well-known variant of PSO, for starch foam materials. In the proposed model, the parameters of the RBF ANN (connection weights, biases, and hidden centers) were optimized by the BBPSO algorithm with an adaptive disturbance factor. This disturbance factor, a re-initialization operator, could prevent the algorithm from trapping into a local optimum, and a better prediction model could be established.

THEORY

Bare-Bones Particle Swarm Optimization with Adaptive Disturbance Factor (BBPSO-AD) Algorithm

The PSO algorithm is a typical heuristic swarm intelligence algorithm. In the search process of the standard PSO algorithm, each particle can be viewed as a potential solution to the problem. The particle velocity and position updating formulas are as follows[26]:

$$v_{i,d}^{k+1}=\omega v_{i,d}^{k}+c_1\left(p_{i,d}^{k}-x_{i,d}^{k}\right)+c_2\left(p_{g,d}^{k}-x_{i,d}^{k}\right) \quad (1)$$

$$x_{i,d}^{k+1}=x_{i,d}^{k}+v_{i,d}^{k+1} \quad (2)$$

where i is equal to 1, …, m (where m is the particle number); $x_{i,d}^{k}$ and $v_{i,d}^{k}$ are the location and speed, respectively; ω is the inertial weight; c_1 and c_2 are the accelerating factors; and $p_{i,d}^{k}$ and $p_{g,d}^{k}$ are the local extreme value and the global extreme value, respectively.

However, the standard PSO algorithm has a premature convergence problem, and it fails to achieve the optimal solution at every execution.[27,28] To improve the premature convergence problem and the easy catching in local extremum of the PSO algorithm, many variants have been proposed. BBPSO is a well-known variant of the PSO algorithm; it gets rid of the traditional velocity equation of PSO. Compared to the traditional PSO, the BBPSO is probably the simplest version PSO because it involves no inertial weight, acceleration coefficient, or velocity. Because of its simplicity and effectiveness, it is natural to extend or apply the BBPSO to some real problems. The updated expression of the standard BBPSO is[29]

$$x_{i,d}^{k+1}=\begin{cases} g_{i,d}^{k}+\sigma_{i,d}^{k}N(0,1) & rand<1 \\ pb_{i,d}^{k}, & \text{otherwise} \end{cases}$$

$$g_{i,d}^{k}=0.5\left(pb_{i,d}^{k}+gb_{i,d}^{k}\right)$$

$$\sigma_{i,d}^{k}=\left|pb_{i,d}^{k}-gb_{i,d}^{k}\right| \quad (3)$$

where $g_{i,d}^{k}$ is the mean of local extreme value and global extreme value, and $\alpha_{i,d}^{k}$ is the deviation of local extreme value and global extreme value, $N(0,1)$ is the Gaussian distribution, $pb_{i,d}^{k}$ is the best position of the ith particle, and $gb_{i,d}^{k}$ is the best global position of the ith particle.

Although the BBPSO has shown potentials to solve different real problems, it is still challenged by premature convergence. In other words, it is very likely to converge to a false global optimum. To improve the search efficiency, an improved BBPSO based on an adaptive disturbance factor was proposed; it was called the BBPSO-AD. The updated strategy is:

$$x_{i,d}^{k+1}=\begin{cases} g_{i,d}^{k}+\sigma_{i,d}^{k}N(0,1) & rand<0.5 \\ x_{i,d}^{k}, & \text{otherwise} \end{cases}$$

$$g_{i,d}^{k}=0.5\left(pb_{i,d}^{k}+gb_{i,d}^{k}\right)$$

$$\sigma_{i,d}^{k}=\left|pb_{i,d}^{k}-gb_{i,d}^{k}\right|+\tau$$

$$\tau=r\left|pb_{s1,d}^{k}-pb_{s2,d}^{k}\right|\times\exp\left\{f[G_b(t)]-f[X_i](t)\right\} \quad (4)$$

where τ is a disturbance factor; $G_b(t)$ is the global extreme value, and $X_i(t)$ is the position of i-th particle, r is a random number within [0,1]; $pb_{s1,d}^{k}$ and $pb_{s2,d}^{k}$ are two bests values, which were chosen randomly from other particles; and f is the optimized objective function.

With the adaptive disturbance factor, each particle has its own disturbance, the value of which changes according to its convergence degree and the diversity of the swarm. Different particles may have different disturbance values even when they are in the same iteration. At the end of our algorithm, the disturbance value converged to zero to ensure the convergence of the swarm. Compared with the standard BBPSO, we adopted the adaptive approach to adjust the value of τ on the basis of the differential fitness value of the current global best position and the differential values of two randomly selected best positions instead of taking a constant value. When the particle has the same fitness as the global best, this particle will be affected by a disturbance with maximal magnitude. In this case, this disturbance, serving as a re-initialization operator, may have prevented the algorithm from trapping into a local optimum. The effect of the disturbance was enhanced with decreasing differential fitness value; this was reflected by the shrinking of the disturbance value. At the end of BBPSO-AD, the disturbance converged to zero because all of the best values converged to one position. As one of the necessary conditions, this ensured the convergence of the swarm.

BBPSO-AD RBF ANN Model

The RBF ANN model is one of the mostly used forward neural network models. Because it can approach any nonlinear function and has good generalization, it has been applied successfully for

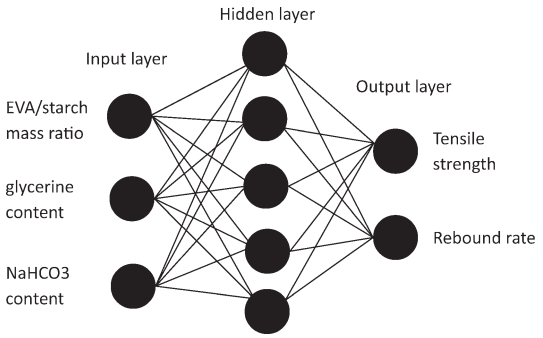

Figure 1. Schematic architecture of the BBPSO-AD RBF ANN for the prediction of starch-based foam materials.

modeling in various fields.[30] The RBF ANN has an input layer, a hidden layer, and an output layer. In this study, the Gaussian function was used as the activation function[31,32]:

$$g_i(x_k)=\exp\left(-\frac{||x_k-c_i||^2}{\sigma_i^2}\right) \quad (5)$$

where $g_i(x_k)$ is the output of the activation function, x_k $(1\le k\le n)$ is the kth output vector; x_k $(1\le k\le n)$ is the kth output vector, c_i $(1\le i\le c)$ is the center of basis function, σ_i is the spreading constant, n is the sample number, and c is the hidden nodes number. The output of the network (O) is as follows:

$$O(x_k)=\sum_{i=1}^{c} w_i g_i(x_k) \quad (6)$$

where w_i is the connection weight.

However, the RBF ANN has various problems. For example, the performance is directly correlated with the optimization of network weights. Research has found that the training process could be viewed as the optimization of the basis function center, expansion constant, and connection weight, that is, the optimization of c_i, σ_i, and w_i. Therefore, an RBF ANN model based on the BBPSO-AD is proposed in this article. In this model, three parameters were optimized by the BBPSO-AD. Therefore, the particle structure [Particle(i)] was as follows:

$$\text{Particle}(i) = [W_{h,o},\ B_{h,o}, C_{\text{basis}-\text{fun}}] \quad (7)$$

where $W_{h,o}$ $(1\le h\le c)$ is the weight matrix, $B_{h,o}$ $(1\le o\le p)$ is the deviation matrix, $C_{\text{basis-fun}}$ is the center of basis function, and p is the output number.

MODEL ESTABLISHMENT

The experimental data in this article are the experimental results from the existing literature.[17] The experiment in this reference used the $L_{16}(4^5)$ orthogonal test method, the crosslinking agent was EVA–starch, the plasticizer was glycerin, the foaming agent was $NaHCO_3$, and the tensile strength and rebound rate of the foaming material were tested as research targets.

After a comprehensive evaluation of the experimental data, a database containing 16 data points was finally established. (details of the experimental data were introduced in Ref. 17). The data were divided randomly into two subsets, including training and testing sets. To verify the network generalization, 11 (ca. 70%) and 5 (ca. 30%) data points were used to train and test, respectively.

In this study, a three-layer RBF ANN model trained by the BBPSO-AD algorithm for the performance prediction of starch-based foam materials was established and called the BBPSO-AD RBF ANN. In accordance with the experimental data, the input of the BBPSO-AD RBF ANN model should contain these experimental variables, and the output should contain the variables of the research target. Therefore, in this study, the input layer had three nodes, namely, the EVA–starch mass ratio, glycerin content, and $NaHCO_3$ content. The input layer showed influencing factors of the study object of the model.

The output layer was the performance factors of the research goal of the model and had two nodes in this study, the tensile strength and the rebound rate of the foam materials. The architecture of the model is shown in Figure 1.

The number of nodes in a hidden layer is generally determined by a formula method or a trial-and-error method. In this study, we combined them together. First, we estimated the number of nodes in the hidden layer by the formula $2\sqrt{mn}+1$ (where m and n are the numbers of nodes in the input layer and the output layer, respectively). Second, we determined the optimal number of nodes through the trial-and-error method. Because the established model had three input nodes and two output nodes, the number of nodes in the hidden layer was calculated to be five. Then, we performed a trail-and-error test by increasing the number of nodes in the hidden layer from 2 to 10. The relation curve between the prediction error and number of nodes in the hidden layer is shown in Figure 2.

As shown in Figure 2, with increasing number nodes in the hidden layer, the mean square error (MSE) decreased first and then increased. The error reached the minimum and the model achieved the best structure (3–5–2) when there were five nodes in the hidden layer.

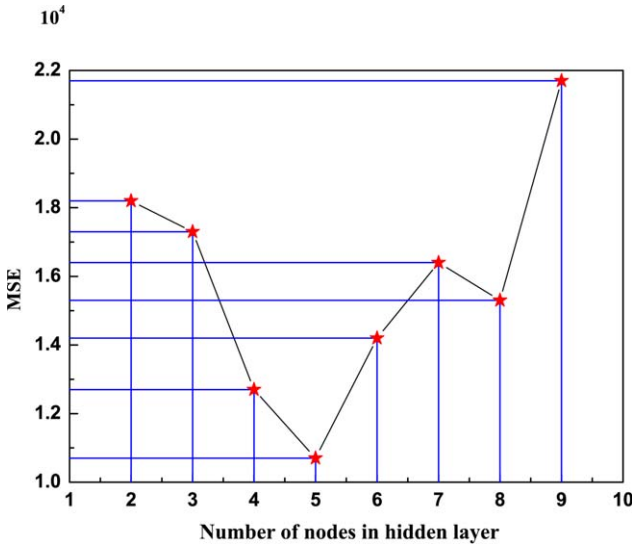

Figure 2. Results of the topology studies for the optimal model. [Color figure can be viewed in the online issue, which is available at wileyonlinelibrary.com.]

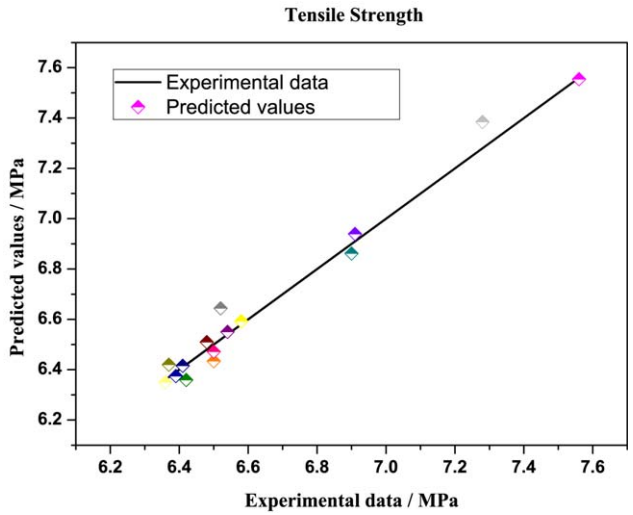

Figure 3. Comparison of the experimental and predicted values of the tensile strength in the training process. [Color figure can be viewed in the online issue, which is available at wileyonlinelibrary.com.]

The performance of this model was validated by three parameters: average relative deviation (ARD), root mean square error of prediction (RMSEP), and squared correlation coefficient (R^2):

$$\mathrm{ARD}=\frac{1}{N}\sum_{i=1}^{N}\frac{|\bar{y}_i-y_i|}{y_i} \tag{8}$$

$$\mathrm{RMSEP}=\sqrt{\frac{1}{N}\sum_{i=1}^{N}\left(y_i-\bar{y}_i\right)^2} \tag{9}$$

$$R^2=\frac{\left[\sum_{i=1}^{N}\left(y_i-y_{\mathrm{ave}}\right)\left(\bar{y}_i-\bar{y}_{\mathrm{ave}}\right)\right]}{\sum_{i=1}^{N}\left(y_i-y_{\mathrm{ave}}\right)^2\sum_{i=1}^{N}\left(\bar{y}_i-\bar{y}_{\mathrm{ave}}\right)^2} \tag{10}$$

where N is the number of sample data; $\bar{y}_i$ is the model predicted value; y_i is experimental value; and y_{ave} and $\bar{y}_{\mathrm{ave}}$ are means of the experimental and predicted data, respectively.

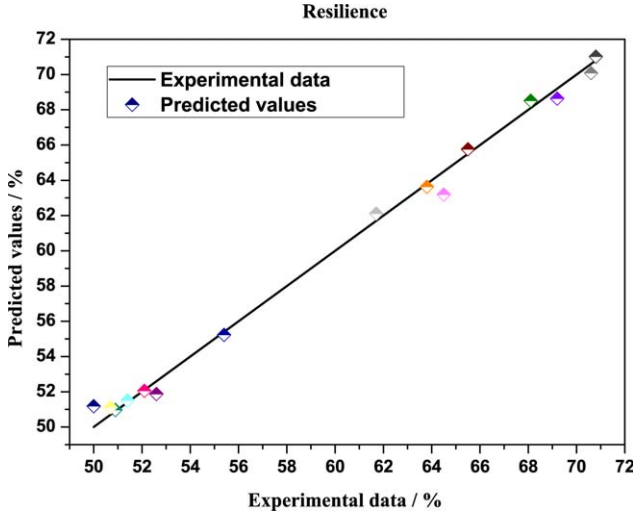

Figure 4. Comparison of the experimental and predicted values of the rebound rate in the training process. [Color figure can be viewed in the online issue, which is available at wileyonlinelibrary.com.]

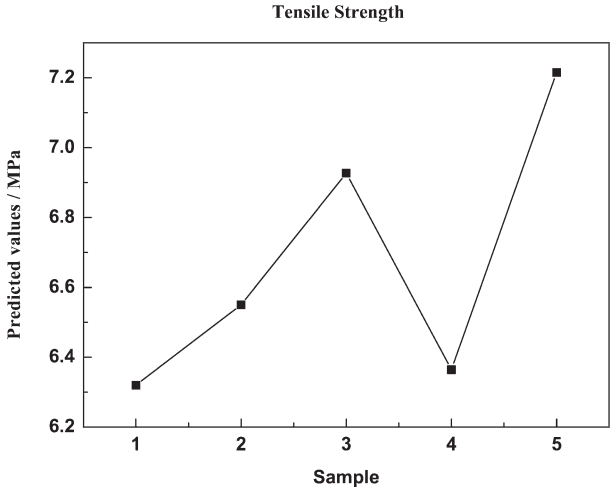

Figure 5. Comparison of the experimental and predicted values of the tensile strength during the test.

RESULTS AND DISCUSSION

Results of the Proposed Model

In this study, a 3–5–2 BBPSO-AD RBF ANN prediction model was established. It includes three nodes in the input layer (EVA–starch mass ratio, glycerin content and $NaHCO_3$ content), five nodes in the hidden layer and two nodes in the output layer (tensile strength and rebound rate).

The established model was trained and tested. Comparisons between the tested and predicted tensile strengths and rebound rates during the training process are shown in Figures 3 and 4.

A straight line represents an ideal model whose predictions are equal to experimental values. A round line represents model predictions, and the vertical distance between the round and straight lines is the absolute error between the predicted value and the experimental results. Obviously, the predicted tensile strength and rebound rate by the model were very close to the experimental values and showed good accordance. As shown by the vertical distance between the round and straight lines, the

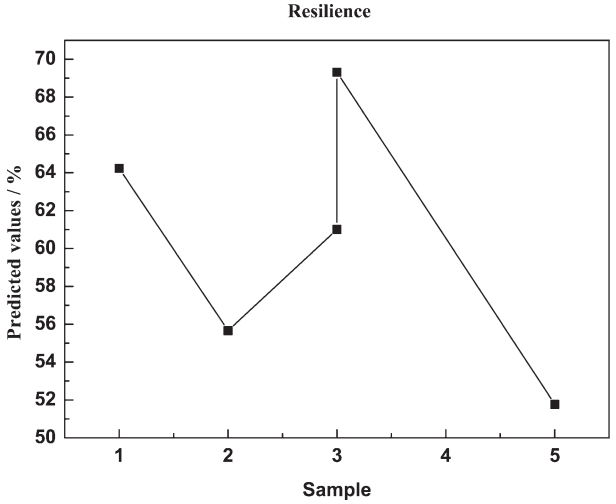

Figure 6. Comparison of the experimental and predicted values of the rebound rate in the testing set.

Table I. Values of ARD, R^2, and RMSEP in the Testing Set

	ARD	RMSEP	R^2
Tensile strength	0.1143	0.0206	0.9873
Resilience	0.1089	0.0119	0.9893
Average	0.1116	0.01625	0.9883

model had a small prediction error and a high prediction accuracy. Figures 5 and 6 show the comparative curves of the tensile strength and rebound rate between the experimental values and model predictions in the testing set.

The test results demonstrated that the tensile strength and rebound rate predicted by the model were in good accordance with the experimental values; this indicated that the prediction was reliable and accurate. Statistics on the evaluation parameters of the prediction model during testing are shown in Table I.

The model showed good prediction performances as viewed from its prediction accuracy and correlation. This confirmed that the established model was competent for studying the related performances of starch-based foam materials.

Comparison of the Proposed Model with Others

To validate the combination properties of the proposed model, we compared it with several models, including the BP ANN, RBF ANN, PSO RBF ANN, and BBPSO-AD RBF ANN models and support vector machine method.[33,34] The convergence curves of each ANN model are shown in Figure 7.

In Figure 7, the convergence rate of each model sped up in a proper order. The BBPSO-AD RBF ANN model approximately finished convergence at the 60th iteration, and the PSO RBF ANN model also became stable at the 100th iteration. The proposed model was superior to the others in terms of the convergence rate and convergence precision.

To show the prediction performances of different models, the tensile strength and rebound rate predicted by different models were compared with the experimental values (Figures 8 and 9).

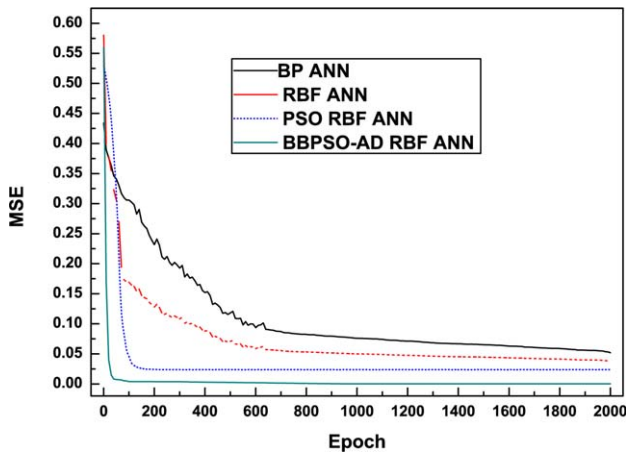

Figure 7. Convergence curves of each ANN model. [Color figure can be viewed in the online issue, which is available at wileyonlinelibrary.com.]

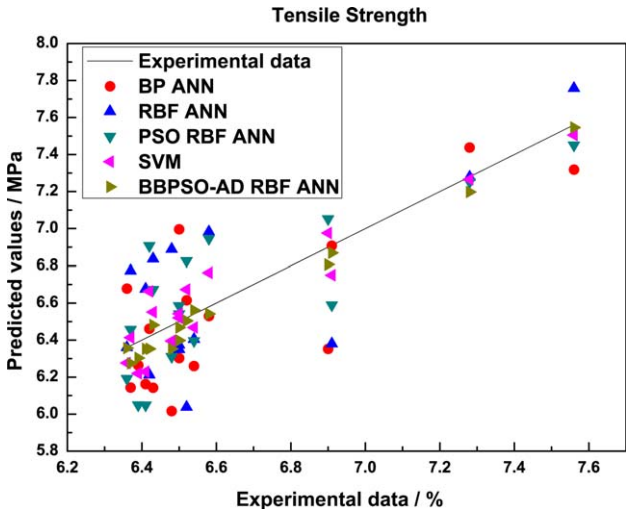

Figure 8. Comparison of the experimental and predicted values of the tensile strength. [Color figure can be viewed in the online issue, which is available at wileyonlinelibrary.com.]

According to the distance between the predicated data point and the straight line, the proposed model showed smaller prediction errors than the others. This was manifested by the fact that most of the predicted data points were near the straight line, and the predicted values were nearly identical to the experimental values.

The statistical data of these models are listed in Table II, and this showed that the proposed model had a significantly higher prediction accuracy and correlation than others.

Discussion

On the basis of the comparison of different models, the proposed model was significantly superior to others in terms of performance, predication accuracy, and correlation. This is because it adopted the BBPSO-AD with a rapid convergence

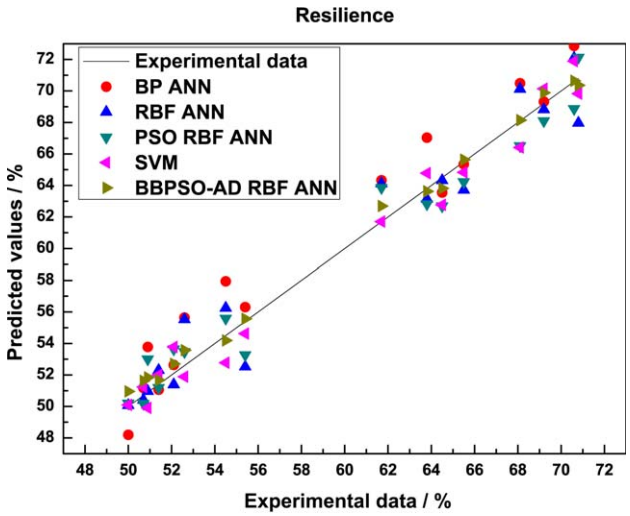

Figure 9. Comparison of the experimental and predicted values of the rebound rate. [Color figure can be viewed in the online issue, which is available at wileyonlinelibrary.com.]

Table II. Statistical Parameters of the Comparison Models

	Resilience			Tensile Strength			Average		
Model	ARD	R^2	RMSEP	ARD	R^2	RMSEP	ARD	R^2	RMSEP
BP ANN	0.4572	0.9297	0.0976	0.3012	0.9267	0.0985	0.3792	0.9282	0.0981
RBF ANN	0.3993	0.9476	0.0765	0.2965	0.9401	0.0778	0.3479	0.9439	0.0772
PSO RBF ANN	0.2718	0.9621	0.0512	0.2616	0.9602	0.0435	0.2667	0.9612	0.0474
Support vector machine	0.2548	0.9678	0.0465	0.2540	0.9667	0.0421	0.2544	0.9673	0.0443
BBPSO-AD RBF ANN	0.1121	0.9879	0.0201	0.2017	0.9866	0.0311	0.1569	0.9873	0.0256

speed as the training algorithm and improved the problem of the prematurity of the algorithm through an adaptive disturbance factor.

The effects of the glycerin content and $NaHCO_3$ content on the tensile strength of the foam material are displayed in Figures 10 and 11. As shown in Figure 10, the tensile strength of the

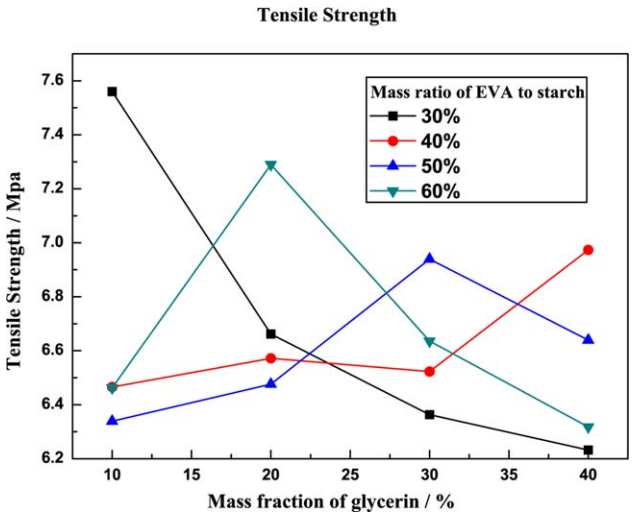

Figure 10. Effects of the glycerin content on the tensile strength. [Color figure can be viewed in the online issue, which is available at wileyonlinelibrary.com.]

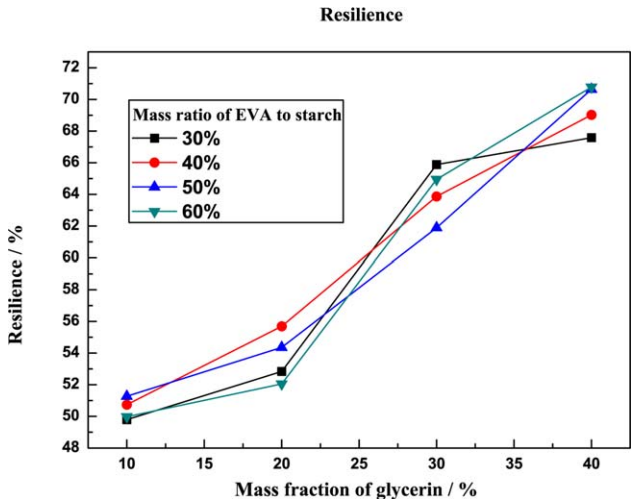

Figure 12. Effects of the glycerin content on the rebound rate. [Color figure can be viewed in the online issue, which is available at wileyonlinelibrary.com.]

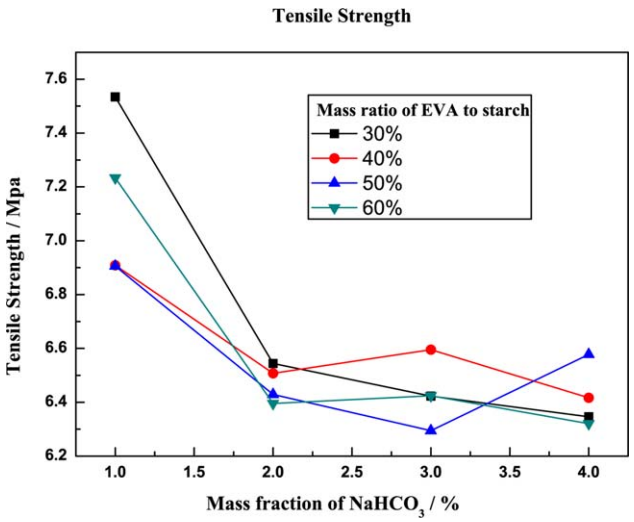

Figure 11. Effects of the $NaHCO_3$ content on the tensile strength. [Color figure can be viewed in the online issue, which is available at wileyonlinelibrary.com.]

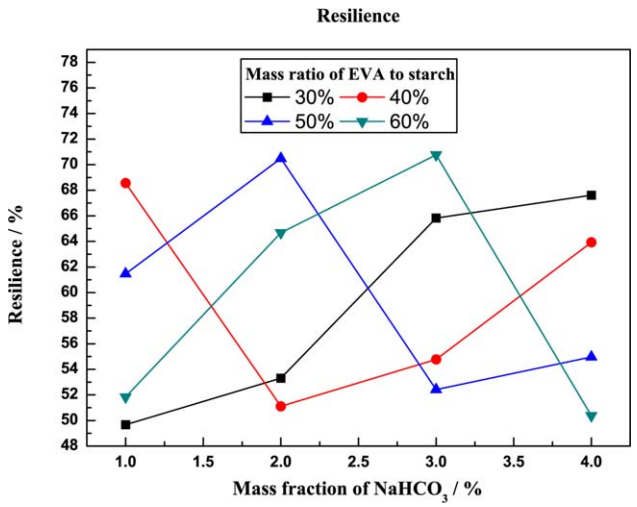

Figure 13. Effects of the $NaHCO_3$ content on the rebound rate. [Color figure can be viewed in the online issue, which is available at wileyonlinelibrary.com.]

starch-based foam material decreased slowly with increasing glycerin content when the mass ratios of EVA to starch were 40 and 50%. As the glycerin content increased, the molecular flow of the material was enhanced; this reduced the mechanical properties of the material. When the mass ratios of EVA to starch were 30 and 60%, there were no uniform trends. As shown in Figure 11, the tensile strength of the starch-based foam material decreased first and then increased with increasing $NaHCO_3$ content, reaching a minimum at about 3% $NaHCO_3$. Under a low $NaHCO_3$ content, with increasing $NaHCO_3$ content, the number of bubbles in the foam material increased because of the foaming agent, whereas the contact area between the bubbles and stress decreased; this reduced the tensile strength. When the $NaHCO_3$ content was saturated, excessive bubbles expanded the contact areas between the bubbles and, thus, resulted in a small increase in the tensile strength. The relation curves of the glycerin content and $NaHCO_3$ content and the rebound rate of the foam material are presented in Figures 12 and 13.

As shown in Figure 12, the rebound rate of the starch-based foam material increased continuously with increasing glycerin content. This was because glycerin formed hydrogen bonds with the hydroxyls of starch and EVA and, thus, weakened molecular interaction, softened the molecular chain, and increased the elasticity. However, the excessive glycerin content caused a high rebound rate and influenced the mechanical properties of the material. In Figure 13, the rebound rate shows a gentle inverted V-shaped variation with increasing $NaHCO_3$ content. The rebound rate increased when the $NaHCO_3$ content increased from 0 to 3%, but it decreased when the $NaHCO_3$ content was higher than 3%. The theoretical reason was that under a small $NaHCO_3$ content, the foaming agent generated bubbles, and the appropriate number of bubbles increased the deformation recovery under pressure. This increased the rebound rate. When there was a high content of $NaHCO_3$, this produced excessive bubbles, and this expanded the contact area between the bubbles. The bubbles were arranged irregularly. Under the effect of pressure, the material deformation could not be recovered, and this decreased the rebound rate.

CONCLUSIONS

The performance prediction model of the starch-based foam material based on the BBPSO-AD RBF ANN could accurately predict its tensile strength and rebound rate. The predicted values were in good accordance with the experimental values and showed a high correlation coefficient.

The predicted values were in good accordance with the experimental values.

1. The tensile strength of the starch-based foam material decreased slowly with increasing glycerin content.
2. The tensile strength decreased first and then increased with increasing $NaHCO_3$ content and reached a minimum at about 3% $NaHCO_3$.
3. The rebound rate was positively correlated with the glycerin content.
4. The rebound rate increased slowly at first and then decreased slowly with increasing $NaHCO_3$ content.

These agree with the variation laws of the experimental results.

The proposed model could provide theoretical support for the selection of technological parameters for the processing of starch-based foam material and could provide a new idea for predicting the properties of other materials.

ACKNOWLEDGMENTS

The authors gratefully acknowledge the support of the National Natural Science Foundation of China (contract grant numbers 51377025 and 51463015) and the Science and Technology Research Project of the Education Department of Jiangxi Province (contract grant numbers GJJ151012 and GJJ150983).

REFERENCES

1. Kaisangsri, N.; Kerdchoechuen, O.; Laohakunjit, N. *Carbohydr. Polym.* **2014**, *110*, 70.
2. Soykeabkaew, N.; Thanomsilp, C.; Suwantong, O. *Compos. A* **2015**, *78*, 246.
3. Gu, R. J.; Sain, M.; Konar, S. *J. Mater. Sci.* **2014**, *49*, 3125.
4. Ge, C. F.; Lansing, B.; Aldi, R. *J. Appl. Polym. Sci.* **2015**, *132*, DOI: 10.1002/app.41904.
5. Cerny, M.; Chlup, Z.; Strachota, A.; Svitilova, J.; Schweigstillova, J.; Halasova, M.; Ryglova, S. *J. Eur. Ceram. Soc.* **2015**, *35*, 3427.
6. Wang, J. J.; Ren, Q.; Zheng, W. G.; Zhai, W. T. *Ind. Eng. Chem. Res.* **2014**, *53*, 1422.
7. Craveiro, R.; Martins, M.; Santos, G. B.; Correia, N.; Dionisio, M.; Barreiros, S.; Duarte, A. R. C.; Reis, R. L.; Paiva, A. *RSC Adv.* **2014**, *4*, 17161.
8. Yang, Z. G.; Graiver, D.; Narayan, R. *Polym. Eng. Sci.* **2013**, *53*, 857.
9. Rodriguez-Perez, M. A.; Simoes, R. D.; Roman-Lorza, S.; Alvarez-Lainez, M.; Montoya-Mesa, C.; Constantino, C. J. L.; de Saja, J. A. *Polym. Eng. Sci.* **2012**, *52*, 62.
10. Soykeabkaew, N.; Supaphol, P.; Rujiravanit, R. *Carbohydr. Polym.* **2004**, *58*, 53.
11. Teixeira, E. D.; de Campos, A.; Marconcini, J. M.; Bondancia, T. J.; Wood, D.; Klamczynski, A.; Mattoso, L. H. C.; Glenn, G. M. *RSC Adv.* **2014**, *4*, 6616.
12. Zhang, Y. Q.; Chang, Z. D.; Luo, W. L.; Gu, S. N.; Li, W. J.; An, J. B. *Chin. J. Chem. Eng.* **2015**, *23*, 276.
13. da Silva, A.; Nievola, L. M.; Tischer, C. A.; Mali, S.; Faria-Tischer, P. C. S. *J. Appl. Polym. Sci.* **2013**, *130*, 3043.
14. Abinader, G.; Lacoste, C.; Le Baillif, M.; Erre, D.; Copinet, A. *J. Cell. Plast.* **2015**, *51*, 31.
15. Rodriguez-Perez, M. A.; Simoes, R. D.; Constantino, C. J. L.; de Saja, J. A. *J. Appl. Polym. Sci.* **2011**, *121*, 2324.
16. Chanvrier, H.; Desbois, F.; Perotti, F.; Salzmann, C.; Chassagne, S.; Gumy, J. C.; Blank, I. *Carbohydr. Polym.* **2013**, *98*, 842.

17. Zeng, G.; Sun, G. *Acta Mater. Compos. Sin.* **2014**, *31*, 107.
18. Wang, H. S.; Wang, Y. N.; Wang, Y. C. *Expert Syst. Appl.* **2013**, *40*, 418.
19. Li, M. S.; Huang, X. Y.; Liu, H. S.; Liu, B. X.; Wu, Y.; Xiong, A. H.; Dong, T. W. *Fluid Phase Equilib.* **2013**, *356*, 11.
20. Alexandridis, A.; Chondrodima, E.; Sarimveis, H. *IEEE Trans. Neural Netw. Learn. Syst.* **2013**, *24*, 219.
21. Mirjalili, S.; Hashim, S. Z. M.; Sardroudi, H. M. *Appl. Math. Comput.* **2012**, *218*, 11125.
22. Qasem, S. N.; Shamsuddin, S. M.; Hashim, S. Z. M.; Darus, M.; Al-Shammari, E. *Inform. Sci.* **2013**, *239*, 165.
23. Li, M. S.; Huang, X. Y.; Liu, H. S.; Liu, B. X.; Wu, Y. *J. Appl. Polym. Sci.* **2013**, *130*, 3825.
24. Zhang, Z. B.; Jiang, Y. Z.; Zhang, S. H.; Geng, S. M.; Wang, H.; Sang, G. Q. *Appl. Soft Comput.* **2014**, *18*, 167.
25. Zhang, Y.; Gong, D. W.; Sun, X. Y.; Geng, N. *Soft Comput.* **2014**, *18*, 1337.
26. Wang, L.; Yang, B.; Chen, Y. H. *Inform. Sci.* **2014**, *274*, 70.
27. Nguyen, T. T.; Li, Z. Y.; Zhang, S. W.; Truong, T. K. *Expert Syst. Appl.* **2014**, *41*, 2134.
28. Li, N. J.; Wang, W. J.; Hsu, C. C. J.; Chang, W.; Chou, H. G.; Chang, J. W. *Neurocomputing* **2014**, *124*, 218.
29. Zhang, Y.; Gong, D. W.; Ding, Z. H. *Inform. Sci.* **2012**, *192*, 213.
30. Sermpinis, G.; Theofilatos, K.; Karathanasopoulos, A.; Georgopoulos, E. F.; Dunis, C. *Eur. J. Oper. Res.* **2013**, *225*, 528.
31. Li, M. S.; Huang, X. Y.; Liu, H. S.; Liu, B. X.; Wu, Y.; Wang, L. *J. RSC Adv.* **2015**, *5*, 45520.
32. Tsekouras, G. E. *Neurocomputing* **2013**, *108*, 36.
33. Pal, R.; Kupka, K.; Aneja, A. P.; Militky, J. *Expert Syst. Appl.* **2016**, *49*, 48.
34. Ziaee, H.; Hosseini, S. M.; Sharafpoor, A.; Fazavi, M.; Ghiasi, M. M.; Bahadori, A. *J. Taiwan Inst. Chem. Eng.* **2015**, *46*, 205.